

## Probabilistic model of an offshore monopile foundation taking into account the soil spatial variability

Abdul-Kader El Haj<sup>1</sup>, Abdul-Hamid Soubra<sup>2</sup>, Jamal Fajoui<sup>3</sup>, Tamara Al-Bittar<sup>4</sup>

<sup>1</sup>PhD student, University of Nantes, GeM, UMR CNRS 6183  
Bd. de l'université, CS 70152  
44603 Saint-Nazaire cedex, France

<sup>2</sup>Professor, University of Nantes, GeM, UMR CNRS 6183  
Bd. de l'université, CS 70152  
44603 Saint-Nazaire cedex, France

<sup>3</sup>Associate professor, University of Nantes, GeM, UMR CNRS 6183  
58 Rue Michel Ange  
44 606 Saint-Nazaire cedex, France

<sup>4</sup>Associate professor, Lebanese University, Faculty of Engineering Tripoli  
Al Kobeh, Liban

### Abstract

*The analysis and design of offshore monopile foundations are generally undertaken using deterministic approaches. In this paper, a probabilistic analysis is performed taking into account the soil spatial variability. The aim is to compute the failure probability against exceeding a threshold value on the pile head displacement. The mechanical model employed for the computation of the monopile head displacement is based on 3D numerical simulations making use of Abaqus finite-element software. The soil is assumed to be an elastic perfectly plastic material obeying Tresca failure criterion. The soil undrained cohesion and Young modulus are considered as log-normal random fields.*

*As it is well known, numerical 3D deterministic models of offshore monopile foundations are computationally-expensive and thus they present a great obstacle to the use of the conventional Monte Carlo Simulation (MCS) methodology for the probabilistic analysis. Furthermore, the study of spatially varying soils with small values of the autocorrelation distances significantly increases the computational effort. To overcome this shortcoming, a reliable and efficient probabilistic model called Global Sensitivity Analysis enhanced Surrogate (GSAS) modeling is proposed. This model is based on kriging metamodeling. The essential issues in the classical kriging-based approaches such as the Active learning method combining Kriging and Monte Carlo Simulations MCS (named AK-MCS method) are that both the choice of a 'best new sample' for the enrichment process and the stopping criterion concerning the addition of a new training sample are defined from the perspective of individual responses, which may lead to some extra evaluations of unnecessary added training*

*samples. In the proposed GSAS method, both the convergence criterion and the strategy of selecting new training samples are defined from the perspective of reliability estimate instead of individual responses of MCS samples. Probabilistic numerical results are then presented and discussed.*

*Keywords: monopile, probabilistic analysis, Abaqus, failure probability, kriging.*

## **1. Introduction**

The analysis and design of offshore geotechnical structures are generally performed using deterministic approaches. With these approaches, mean values of the soil properties are used without rigorously taking into account the uncertainties of these parameters and without considering the spatial correlation structure of these properties. Also, mean values of the applied loads are considered in the analysis. The probabilistic approaches, on the contrary, allow one rigorously take into account the uncertainties of the soil properties and the spatial variability of these properties together with the uncertainties related to the applied loads. The outcomes of these approaches may be the statistical moments of the system response or the probability of failure against an acceptable threshold of this system response.

For the probabilistic analyses of offshore geotechnical structures, several authors have considered the effect of the soil spatial variability on the statistical moments of the system response or on the failure probability against a prescribed value of this response. For instance, one may cite among others Li *et al.* (2016) and Li *et al.* (2017) for the bearing capacity of spudcan foundations, Charlton and Rouainia (2017) for the bearing capacity of skirted foundations and Vahdatirad *et al.* (2013) for the problem of a monopile foundation. In this paper, a probabilistic analysis of an offshore monopile foundation subjected to a combined loading was investigated. A soft clayey soil layer with spatially varying soil properties was considered in the analysis.

As it is well known, the three-dimensional numerical deterministic models of offshore monopile foundations are very time consuming because they are based on finite element/finite difference methods. Furthermore, the probabilistic analysis of a very heterogeneous soil layer (i.e. a soil layer with small values of the autocorrelation distances) significantly increases the computation time as compared to the time required for a homogeneous soil layer due to the increase in the stochastic dimension of the treated problem (although the probabilistic analysis of a homogeneous soil layer is by itself computationally expensive).

Because of the two mentioned issues related to the 3D mechanical modeling and the soil spatial variability, the conventional probabilistic method (i.e. Monte Carlo Simulation MCS methodology) is very expensive for the computation of the failure probability. It becomes unaffordable if an accurate value of the failure probability (i.e. with a small value of the coefficient of variation on this failure probability) is desired. Consequently, a more advanced probabilistic approach is needed.

Recently, several kriging-based metamodeling approaches (e.g. AK-MCS, AK-IS, etc.) have been developed [see Echard et al. (2011, 2013)] and were shown to be efficient with respect to the classical MCS methodology as one can obtain an accurate probability of failure needing a smaller number of calls to the mechanical model. Notice however that the essential issues in these approaches are (i) the choice of a best new training sample for the construction of the metamodel and (ii) the stopping criterion related to the addition of a new training sample. Indeed, these issues are defined from the perspective of individual responses. This may lead to some extra evaluations of unnecessary added training samples.

In order to overcome this shortcoming, a Global Sensitivity Analysis enhanced Surrogate (GSAS) modeling was developed by Hu and Mahadevan (2016). Within GSAS, a powerful new stopping criterion was suggested and a new way of selecting a new training sample was proposed. In this regards, both the convergence criterion and the strategy of selecting new training samples are defined from the perspective of reliability estimate instead of individual responses of MCS samples. Indeed, the new training samples are identified according to their contribution to the uncertainty in the reliability estimate and the selection of new training samples stops when the accuracy of the reliability estimate reaches a specific target.

It should be mentioned that Hu and Mahadevan (2016) have validated the proposed method based on several academic examples where the performance function was given by an analytical equation. The aim of this paper is to extend the GSAS approach proposed by Hu & Mahadevan (2016) to the case of random field problems in order to study geotechnical structures involving spatial variability of the soil properties. More specifically, this paper presents a probabilistic analysis at the Serviceability Limit State SLS of a large diameter monopile foundation in a spatially varying clay. The objective is the computation of the failure probability  $P_f$  of exceeding a threshold value on the pile head rotation due to a prescribed applied combined loading. Notice that the soil undrained cohesion was considered as a random field. The soil undrained Young's Modulus was assumed to be linearly related to the soil undrained cohesion. Thus, it is implicitly assumed a random field having the same distribution of the soil cohesion. Only the soil spatial variability in the vertical direction was considered in this paper. The Expansion Optimal Linear Estimation method (EOLE) methodology proposed by Li and Der kiureghian (1993) was used to generate the random field. The mechanical model employed to calculate the system response (i.e. the pile head rotation) was based on numerical simulations using Abaqus finite-element software.

This paper is organized as follows: The first section describes the soil-monopile mechanical model. This is followed by a brief description of the coupled mechanical probabilistic model based on GSAS approach and its application to the case of a large diameter monopile in a spatially varying clayey soil. Some numerical results are then presented and discussed. The paper ends by a conclusion of the main findings.

## 2 Mechanical model of the soil-monopile system

A 3D finite element model of the soil-monopile system has been carried out using the commercial software Abaqus/Standard [ABAQUS (2016)]. Table (1) provides the geometrical and material properties of the monopile. An open-ended steel monopile of 3m diameter was considered in this study. The embedded length,  $L$ , was taken equal to 18 m. The pile was extended of 1.0 m above the seabed to prevent the soil from going over the pile (Kellezi and Hansen 2003). The wall thickness of the pile  $t$  was taken equal to 5 cm, thus respecting the minimum wall thickness required by the API (2000) and provided by the following equation:

$$t = 6.35 + \frac{D}{100} \quad (1)$$

Where  $t$  [mm] is the wall thickness of the monopile and  $D$  [mm] its outer diameter. The steel pile material was assumed to be linear elastic with Young's modulus  $E_p$  of 210 GPa, Poisson's ratio  $\nu_p$  of 0.3 and a density of  $7840 \text{ kg/m}^3$ . Concerning the type of soil used in the numerical modelling, an undrained clayey soil was considered in the analysis. It was assumed to follow the elastic-perfectly plastic Tresca constitutive model which is defined by the undrained cohesion  $C_u$ , the undrained Young's modulus ( $E_u$ ) and the Poisson's ratio ( $\nu_u$ ). In this paper, the soil was assumed to have a saturated unit weight of  $18 \text{ kN/m}^3$  and a Poisson ratio of 0.495. The statistical input data of the soil undrained cohesion and the soil undrained Young's modulus will be given in the next section when dealing with the coupled mechanical probabilistic model.

**Table 1:** Geometrical and material properties of the monopile.

| Outer diameter<br>$D$ (m) | Embedded length $L$<br>(m) | Thickness $t$<br>(m) | Young modulus<br>$E_p$ (GPA) | Poisson ratio<br>$\nu_p$ | Density<br>$\text{kg/m}^3$ |
|---------------------------|----------------------------|----------------------|------------------------------|--------------------------|----------------------------|
| 3.00                      | 18.00                      | 0.05                 | 210                          | 0.3                      | 7840                       |

As it may be seen from Figure 1, an offshore monopile that is subjected to a vertical load  $V$  (representing the structure weight) together with a horizontal force acting at a height  $h$  (supposed equal to 38.6 m above the sea bed level) is considered in the analysis. The moment at mudline level is thus  $M = H \times h$ . In this paper, the vertical and horizontal loads are supposed to be equal to 2 MN and 0,55 MN respectively.

Because of symmetry, only one half of the entire cylindrical soil domain is considered in the analysis. As may be seen from figure 1, the numerical model has a radius of  $10 D$  from the monopile center and a height equal to  $1.6 L$ . It was verified that with these model dimensions, the behavior of the soil-monopile system was not influenced by the artificial boundary effects. Concerning the model boundary conditions, the bottom

of the soil model was fixed against translation in all directions whereas the lateral boundaries were fixed against lateral translation. Also, the symmetrical vertical plane was fixed against translation in the normal direction. The soil mesh was constructed using 8-noded linear brick elements (C3D8). Incompatible mode 8-noded linear brick elements (C3D8I) were used for the monopile in order to accurately simulate the flexural behavior of the pile. An illustration of the adopted mesh is shown in figure 1.

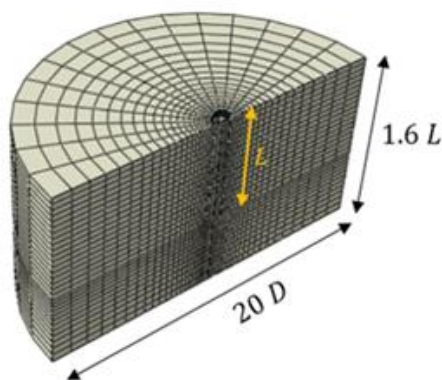


**Figure 1.** Domain and mesh used in the numerical simulations of the soil-monopile system

Surface-to-surface master/slave contact formulation was used to model the interaction between the monopile and the soil. Since the monopile is much stiffer than the soil, it was selected as the master surface while the soil in contact with the monopile was selected as the slave surface. In the normal direction, a linear pressure-overclosure relationship with default parameters was used in order to model the normal behavior. The frictional behavior was modelled using Coulomb friction law: the maximum shear stress at contact was equal to the contact stress multiplied by the friction coefficient  $\mu$  where  $\mu$  was taken equal to 0.24 in this paper. According to Jeong et al. (2004), Lemos and Vaughan (2000), and Tsubakihara and Kishida (1993), this coefficient was found to lie within the range [0.2 - 0.4]. When the shear stress reaches the maximum value, the surfaces slide relative to one another in the tangential direction.

The finite element calculation was executed step-wised. A geostatic step was first performed for the generation of the initial stress state of the soil in the whole model consisting of soil elements only. This is done by defining the vertical total stress components and specifying the coefficient of earth pressure at rest  $K_0 = 1$ , and then running the geostatic step in the presence of the gravity forces in order to reach a first equilibrium with negligible deformations. In a second step, the monopile was simulated by (i) removing the soil elements located at the pile position and generating the steel elements representing the monopile, (ii) activating the contact conditions between the monopile and the soil and (iii) applying the weight of the generated monopile. Finally, in a third step, the horizontal and vertical forces and the corresponding moment are applied in increments at a reference point (taken here as the center of the monopile at the pile head level) where the applied moment was equal to  $M = H \times (h - 1) = 20.68 \text{ MN.m}$ .

For a deterministic calculation at the serviceability limit state using an undrained cohesion  $C_u$  of 50 kPa and an undrained Young's modulus  $E_u$  of 10,000 kPa ( $=200 \times C_u$ ), the obtained value of the monopile rotation at mud-line is equal to  $0.23^\circ$ . This value is slightly lower than the limit rotation value ( $\theta_{SLS} = 0.25^\circ$ ) imposed by the DNV (2014) at the Serviceability Limit State.

### 3 Coupled mechanical probabilistic model

Based on some investigations on the variability of seabed soils, Lacasse and Nadim (1996) found that the undrained cohesion of clay followed a normal or lognormal distribution with a coefficient of variation ranging between 5% and 35%. According to Li et al. (2016), the scale of fluctuation of offshore soils ranges between 7 m and 9000 m in horizontal direction. In vertical direction, the scale of fluctuation is much smaller, ranging between 0.4 m and 7.14 m. As a result, the horizontal variability of the soil was not taken into account in this work for simplicity. It will be investigated in a future work.

The uncertain soil parameters considered in this paper may be described as follows: the undrained soil cohesion  $C_u$  of the clay was modeled by a lognormal random field. A reference configuration with a mean value of 50 kPa, a coefficient of variation of 10% and a vertical autocorrelation distance of 2 m was considered in the analysis. Notice however that several other values of the vertical autocorrelation distance were also investigated in this paper in order to examine the effect of the soil vertical variability on the value of the failure probability. The undrained Young's modulus  $E_u$  was assumed to be linearly related to  $C_u$  such that  $E_u = K_c \times C_u$  (where  $K_c$  was taken equal to 200 in this work). This means that the soil undrained Young modulus was also considered to follow a log-normal random field distribution. Notice finally that  $K_c$  is a correlation factor that is dependent on the clay plasticity index and the over-consolidation ratio OCR [cf. USACE (1990)].

The coupled mechanical probabilistic model used to perform the probabilistic analysis may be described by the following steps:

1. The random fields realizations were first generated using EOLE method [see Li and Der kiureghian (1993)]. It should be noted that a square exponential autocorrelation function was used in the analysis. In one dimension, this autocorrelation function is given by the following equation:

$$\rho = \exp\left(-\left(\frac{|\Delta z|}{a_z}\right)^2\right) \quad (2)$$

where  $a_z$  is the autocorrelation distance in the vertical direction.

2. After the random fields generation, material random properties values were saved as solution-dependent state variables (SDV) and transmitted to the integration points of the soil elements by a User defined material subroutine

UMAT written in Fortran [see Clausen et al. (2007) for more details]. This subroutine was used to define an elastic-perfectly plastic Mohr-Coulomb constitutive model for the soil behaviour since it was not possible to spatially vary the soil strength parameters using the Abaqus built-in Mohr-Coulomb constitutive model. A typical realization of the soil Young modulus random field is shown in Figure 2 (notice that SDV2 in Figure 2 represents the soil Young's modulus).

3. After each mechanical calculation using Abaqus, the post-processing of the mechanical model response was performed using the *Abaqus2Matlab* toolbox [see Papazafeiropoulos et al. (2017)]. This toolbox is a suitable piece of software which is able to connect Abaqus with Matlab. Using this toolbox, the pile nodes displacement values at the mud-line level were read in Matlab and then used to compute the rotation value obtained from each realization.
4. Finally, the response is stored in Matlab and used by the probabilistic GSAS method.

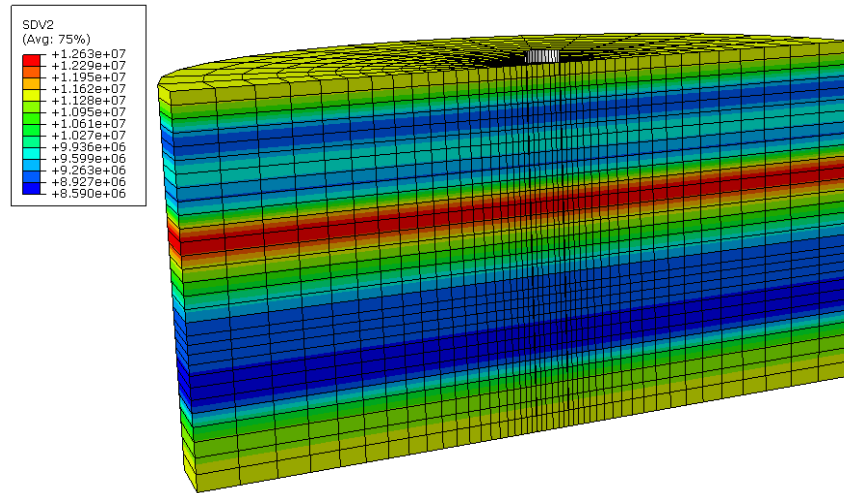


Figure 2. Typical realization of the soil Young modulus

The general procedure of the GSAS method (which may be considered as an improvement of AK-MCS) as adapted to the case of random fields problems can be summarized as follows:

- Generation by Monte Carlo simulation of  $x^{(i)} (i = 1, 2, \dots, N_{MCS})$  samples. In this work,  $N_{MCS}$  was taken equal to 500,000. Each sample  $x^{(i)}$  consists of  $M$  standard Gaussian random variables where  $M$  is the number of random variables needed by EOLE methodology to accurately discretize the cohesion random field. This number will be given later in this paper [see Table 4].
- Random selection of a small design of experiments DoE from the generated population (a DoE of 15 samples was used in this work). Then, use EOLE methodology to transform each sample into realizations of  $C_u$  (and  $E_u$ ) that provide the spatial distribution of the soil undrained cohesion (and Young

modulus). For each selected sample, the performance function  $G$  is evaluated using the following equation:

$$G = \frac{\theta_{SLS}}{\theta} - 1 \quad (3)$$

where  $\theta_{SLS} = 0.25^\circ$  is the limit rotation value at the Serviceability Limit State [see DNV (2014)] and  $\theta$  is the pile rotation at mudline computed based on the Abaqus model.

- Based on the DoE and the corresponding performance function evaluations, an approximate kriging meta-model is constructed in the standard space of random variables using the DACE toolbox [Lophaven et al. (2002)].
- For each Monte Carlo sample  $x^{(i)}$ , the random response predicted by the approximate kriging surrogate model is a Gaussian variate as follows:

$$G_p(x^{(i)}) \sim N(g(x^{(i)}), \sigma_{G_p}^2(x^{(i)}))$$

where  $g(x^{(i)})$  and  $\sigma_{G_p}^2(x^{(i)})$  are the mean prediction and the corresponding mean square error (kriging variance) respectively. The kriging predictions values  $g(x^{(i)})$  (mean values) and their corresponding kriging variance  $\sigma_{G_p}^2(x^{(i)})$  values are determined for the whole MCS samples using the DACE toolbox. Then the failure probability  $P_f$  is estimated using equation (4) after replacing the meta-model random responses  $G_p(x^{(i)})$  by the mean prediction values  $g(x^{(i)})$ .

$$P_f = \sum_{i=1}^{N_{MCS}} I(G_p(x^{(i)})) / N_{MCS} \quad (4)$$

In this equation,  $I(G_p(x^{(i)})) = 1$  if  $G_p(x^{(i)}) \leq 0$ , otherwise,  $I(G_p(x^{(i)})) = 0$  where  $x^{(i)} (i=1, 2, \dots, N_{MCS})$  are the sampling points from MCS. Thus,  $P_f$  is estimated by counting the number of negative mean predictors and dividing it by the total number of MCS samples. The corresponding coefficient of variation  $COV(P_f)$  is given by the following equation:

$$COV(P_f) = \sqrt{\frac{1 - P_f}{P_f \cdot N_{MCS}}} \quad (5)$$

- It should be emphasized here that the value of the failure probability computed at this stage is far from being accurate because of the small DoE used so far. An enrichment process is thus needed. Within AK-MCS approach, the best next candidate sample adopted during the enrichment process is selected as the one that is the most close to the limit state surface. This sample could be considered

as the one that mostly reduces the uncertainty in  $P_f$  if the sample responses  $G_p(x^{(i)})$  predicted from the surrogate model were completely independent. Notice however that these sample responses are correlated normal variables according to the property of the kriging model. The GSAS approach allows one to overcome this shortcoming. The basic idea of this approach is to treat the probability of failure estimate  $P_f$  as a random variate representing the output of the system presented in Figure 3 where the system inputs are the random responses  $G_p(x^{(i)})$  predicted by the kriging meta-model. In other words, the uncertainty in the input random variates  $G_p(x^{(i)})$  is propagated through the system given by equation (4) and thus, the uncertainty in the failure probability estimate can be quantified.

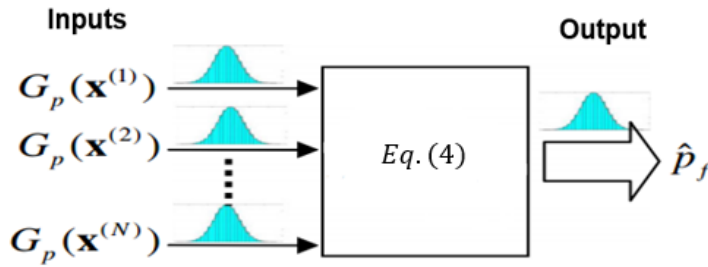


Figure 3. Probability of failure estimate as a system response

For an efficient enrichment of the kriging meta-model within GSAS, the new training sample is selected based on its contribution to the uncertainty of the quantity of interest (i.e.  $P_f$ ). It should reduce the uncertainty in  $P_f$  in the most significant way. This is done *via* a global sensitivity analysis method extended to the case of models with dependent inputs. The extended FAST method developed by Xu and Gertner (2007) was used in this paper. The enrichment process within GSAS approach can be briefly described as follows:

The MCS samples are firstly classified into two groups according to their  $U$  values where  $U$  is a learning function usually employed in the kriging-based approaches. It is given by the following equation:

$$U(x^{(i)}) = \frac{|g(x^{(i)})|}{\sigma_{G_p}(x^{(i)})} \quad (6)$$

Notice that a large value of  $U$  indicates a low probability of making an error on the sign of  $g(x)$ . For  $U(x) > 2$ , the probability of making a mistake on the sign of the performance function value is less than 0.023 [Echard et al. (2011)]. Based on that, the MCS samples  $x^{(i)} (i = 1, 2, \dots, N_{MCS})$  are divided into two groups: The group  $x_{g1}^{MCS}$  with  $U$  values larger than 2 and the group  $x_{g2}^{MCS}$  with

the remaining samples in  $x^{MCS}$ . The global sensitivity analysis is then performed on the  $x_{g2}^{MCS}$  group samples to determine their contributions to the uncertainty of  $P_f$  since we assume that the uncertainty of  $P_f$  comes from this group of samples. It should be noted that in order to reduce the dimensionality of the problem, only a reduced number  $n_{can}$  of samples (taken equal to 20 in this work) of the  $x_{g2}^{MCS}$  group with the lowest  $U$  values are selected to perform the global sensitivity analysis since they have high probability of having wrong performance function signs (i.e. high probability of being the new selected training sample).

- A powerful stopping criterion based on the quantification of the uncertainty in the failure probability was suggested within GSAS approach. Although a prescribed maximal value of the uncertainty on the failure probability would be a quite relevant stopping condition (because it makes sure that the uncertainty in  $P_f$  is sufficiently small), Hu and Mahadevan (2016) suggest stopping the addition of new samples based on the uncertainty of the error on the failure probability  $\varepsilon_r$ . The error on the failure probability is a measure of the error between the theoretical and the computed values of the failure probability. It is defined by the following equation:

$$\varepsilon_r = \frac{P_f - \hat{P}_f}{P_f} \quad (7)$$

where  $P_f$  is the theoretical failure probability given by equation (4) and  $\hat{P}_f$  is the estimate value of the failure probability that can be directly computed based on the kriging meta-model mean prediction values  $g(x^{(i)})$ .

It should be noted here that  $P_f$  is not a unique scalar value that can be computed [because  $G_p(x^{(i)})$  in equation 4 is a Gaussian variate], but a random variate for which one can quantify the corresponding uncertainty. The uncertainty in  $\varepsilon_r$  as given by equation (7) was thus quantified herein based on the uncertainty quantification of  $P_f$ . The sampling based method was used: This method consists in generating  $n_r$  samples ( $n_r = 600$  in this work) of  $N_2$  correlated normal variables  $G_p(x_{g2}^{MCS}(i)), i = 1, 2, \dots, N_2$  for each sample where  $N_2$  is the number of samples in the  $x_{g2}^{MCS}$  group. From these samples, one can compute  $n_r$  samples of the failure probability  $P_f$  and other  $n_r$  corresponding samples of the error  $\varepsilon_r$ . From the  $\varepsilon_r(i), i = 1, 2, \dots, n_r$  samples, the Kernel Smoothing function is employed to fit the distribution of the error  $\varepsilon_r$ . Based on the fitted distribution, Hu and Mahadevan (2016) have suggested stopping the addition of new samples when the quantity  $\varepsilon_r^{\max}$  becomes smaller

than a prescribed threshold  $a$  (where  $a$  is taken equal to 0.1% in this paper) where  $\varepsilon_r^{\max}$  is defined as follows:

$$\varepsilon_r^{\max} = \max \left\{ \left| F_{\varepsilon_r}^{-1}(0.99) \right|, \left| F_{\varepsilon_r}^{-1}(0.01) \right| \right\} \quad (8)$$

In this equation,  $F_{\varepsilon_r}^{-1}$  is the inverse CDF of  $\varepsilon_r$ . The proposed stopping condition corresponds to a probability that, the actual estimation error on  $P_f$  is larger than 0.1%, is equal to 0.02. For more information on this criterion, the reader may refer to Hu and Mahadevan (2016).

Notice finally that the value of  $\varepsilon_r^{\max}$  was checked every time the surrogate model was updated except for the case where the number  $N_2$  was too large (>8000 samples). The reason is related to the fact that the error computation cost is very expensive in this case. Furthermore, this cost would be with no interest since the uncertainty on the failure probability estimate is obviously significant.

## 4 Numerical results

### 4.1 Probabilistic numerical results

The probabilistic numerical results are presented in this section for the reference case presented above where the vertical autocorrelation distance was taken equal to 2m.

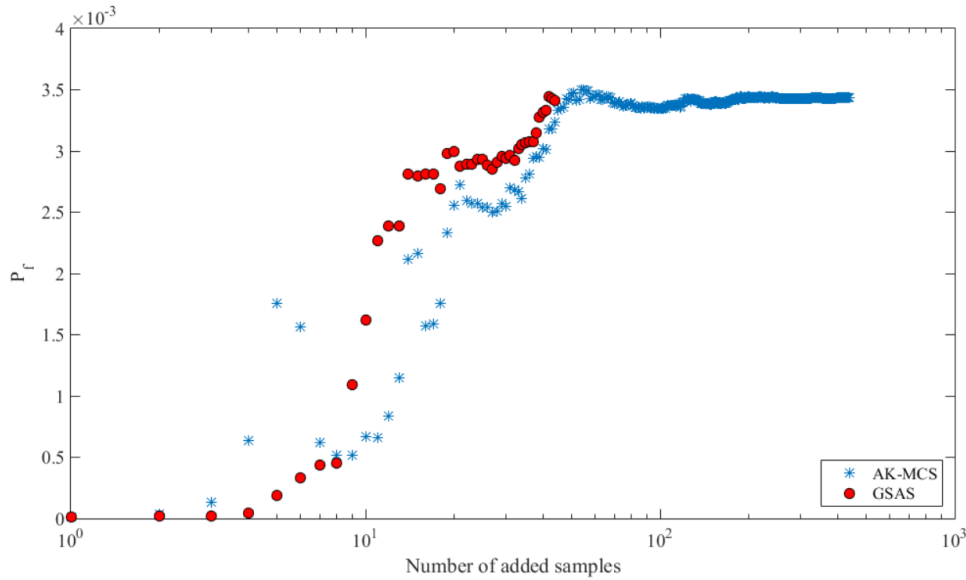


**Figure 4.** Failure probability vs the number of added samples

Figure (4) presents the evolution of  $P_f$  with the number of added samples (as given by GSAS) until reaching the stopping criterion  $\varepsilon_r^{\max} < 0.1\%$ . As may be seen from this figure, the stopping condition was reached for only 44 added samples. For this

number of samples, a failure probability of  $3.41 \times 10^{-3}$  and a corresponding coefficient of variation of 2.42% were obtained.

**Table 2:** Comparison of GSAS and AK-MCS results.

| Method | $\hat{P}_f (\times 10^{-3})$ | %COV( $\hat{P}_f$ ) | Added samples |
|--------|------------------------------|---------------------|---------------|
| GSAS   | 3.41                         | 2.42                | 44            |
| AK-MCS | 3.41                         | 2.42                | 440           |

In order to check the efficiency of GSAS with respect to the classical AK-MCS approach, a probabilistic computation has been performed on the same problem treated in this section but using AK-MCS. Figure (4) presents the failure probability (as obtained by AK-MCS) versus the number of added samples until reaching the classical stopping criterion used in AK-MCS (i.e.  $U > 2$ ). As may be seen from Figure (4) and Table (2), GSAS is a powerful approach since it provides quasi-similar values of the failure probability and the coefficient of variation on this failure probability as AK-MCS making use of a much reduced number of calls to the mechanical model.

Table 3 shows (as was prescribed by the stopping condition) that the error  $\varepsilon_r^{\max}$  becomes smaller than 0.1% for the optimal number of samples suggested by GSAS (44 added samples in this example). This error was not computed before reaching 41 samples (thus reducing the computation time) because of the high values of the uncertainty in  $P_f$  for these cases ( $N_2 > 8000$ ) as mentioned above.

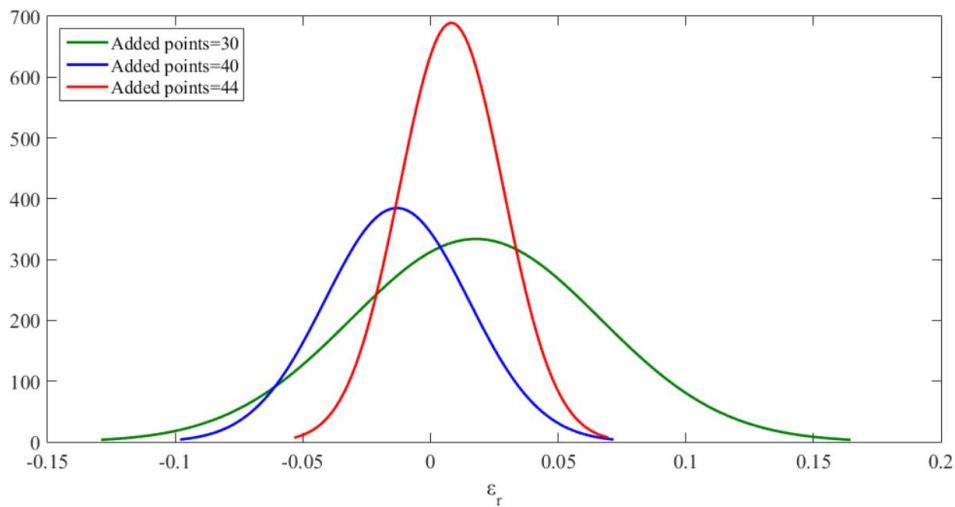
**Table 3:**  $\varepsilon_r^{\max}$  vs the number of added samples

| Number of Added samples | $\varepsilon_r^{\max}$ (%) |
|-------------------------|----------------------------|
| 41                      | 0.23                       |
| 42                      | 0.18                       |
| 43                      | 0.21                       |
| 44                      | 0.08                       |

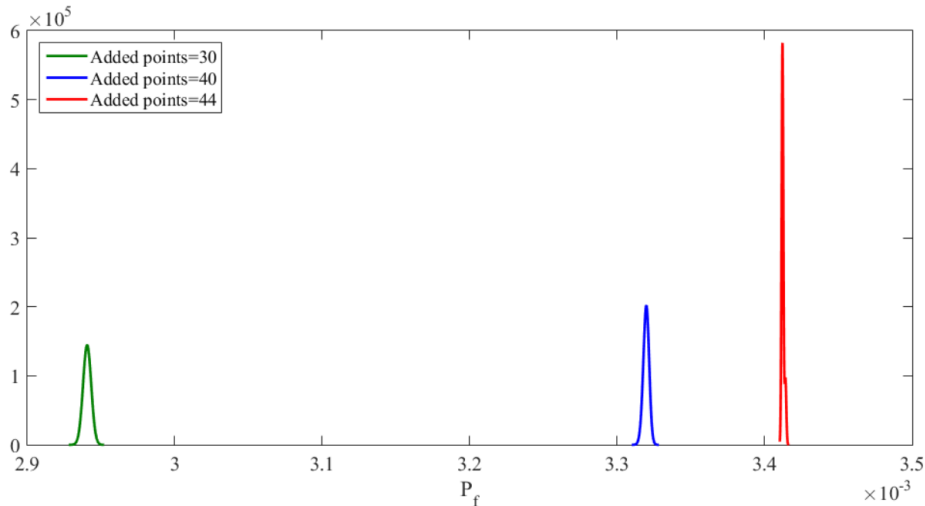
Figure 5 presents the evolution of the distribution of  $\varepsilon_r$  with the number of added samples. This figure shows that (i) the variability of  $\varepsilon_r$  decreases with the number of added samples, the corresponding standard deviation value becomes very small with a value of  $2.03 \times 10^{-4}$  when reaching the optimal number of added samples (i.e. 44 samples) and (ii) the final mean value of the error converges to zero. These two observations provide a quite good indication on the convergence of the estimated failure probability to its theoretical value.

Figure 6 presents the evolution of the distribution of  $P_f$  with the number of added samples. As in Figure 5, one can observe a decrease in the variability of this distribution with the increase in the number of added samples. A very small standard deviation value of  $6.94 \times 10^{-7}$  was obtained when reaching the optimal number of added samples.

The obtained results confirm that the stopping criterion on the error not only makes sure that a small uncertainty on the error was reached but it also leads to a small uncertainty on the computed failure probability.



**Figure 5.** Evolution of the fitted distribution of  $\varepsilon_r$  with the added points



**Figure 6.** Evolution of the fitted distribution of  $\hat{P}_f$  with the added points

The kriging meta-model was expressed in this paper in the standard space of random variables. The computation of the Hasofer-Lind reliability index and the corresponding design point is thus quite straightforward. A minimization of the

reliability index subjected to the constraint that the performance function is equal to zero was performed.

Figure 7 presents the critical realization of the soil Young modulus corresponding to the obtained design point. This figure exhibits some symmetry in the soil Young modulus about the pivot point of the monopile indicated by a red circle in Figure 8.

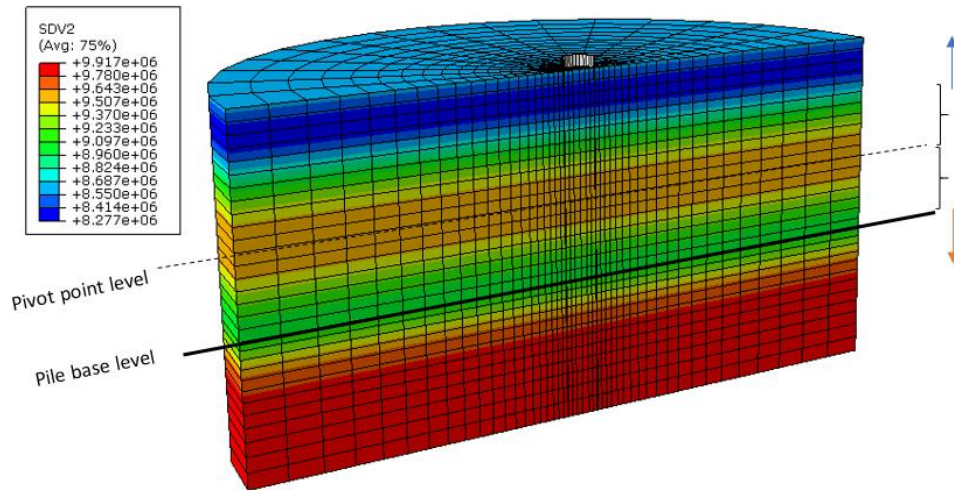


Figure 7. Critical realization of the soil Young modulus

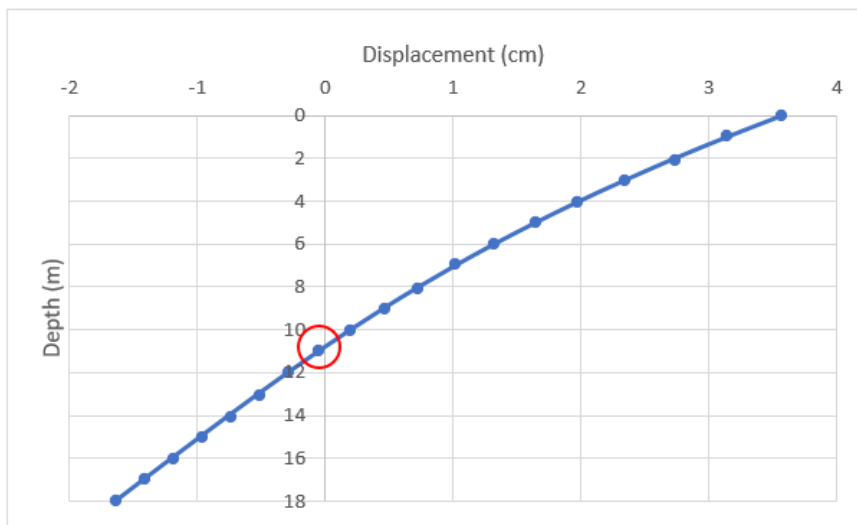


Figure 8. Distribution of the lateral displacement along the pile depth

A close examination of the obtained Young modulus distribution allows one to observe that a weaker soil appears for the depths corresponding to higher horizontal monopile displacements. It should be noted that an increase in the value of the Young modulus was observed below the base of the monopile. This is to be expected since the soil mass under the base has no influence on the monopile horizontal displacements.

## 4.2 Parametric study

In this section, a parametric study was undertaken. The aim is to investigate the effect of the vertical autocorrelation distance on the failure probability at SLS.

Table 4 provides the number of random variables adopted within EOLE methodology and the corresponding value of the variance of the error for different values of the vertical autocorrelation distance. As may be seen from this table, a small value of the variance of the error (smaller than 5%) was adopted for all the configurations treated in this paper. This means that a sufficiently accurate random field discretization was adopted in the analysis.

**Table 4:** Adopted number of random variables and the corresponding value of the variance of error of EOLE together with the values of  $\hat{P}_f$ ,  $COV(\hat{P}_f)$  and number of added realizations for various soil variabilities.

| Correlation length (m) | Adopted number of random variables | Variance of the error % | $P_f (\times 10^{-3})$ | % $COV(\hat{P}_f)$ | Added samples |
|------------------------|------------------------------------|-------------------------|------------------------|--------------------|---------------|
| 2                      | 16                                 | 3.77                    | 3.41                   | 2.42               | 44            |
| 3                      | 11                                 | 3.22                    | 10.4                   | 1.37               | 32            |
| 5                      | 7                                  | 3.22                    | 26.9                   | 0.84               | 34            |
| 12                     | 3                                  | 4.57                    | 69.9                   | 0.51               | 3             |
| 18                     | 3                                  | 0.84                    | 91.8                   | 0.44               | 1             |
| 30                     | 2                                  | 1.27                    | 107.5                  | 0.40               | 1             |
| 50                     | 2                                  | 0.19                    | 114.6                  | 0.39               | 1             |
| 100                    | 1                                  | 1.79                    | 117.5                  | 0.38               | 1             |
| 10000                  | 1                                  | $1.65 \times 10^{-3}$   | 120.6                  | 0.38               | 1             |

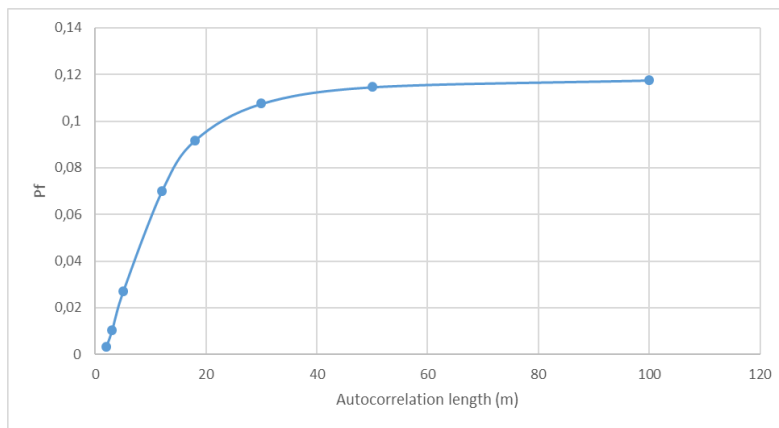


**Figure 9.** Evolution of  $\hat{P}_f$  with the vertical autocorrelation distance

Table 4 and Figure 9 show that the failure probability increases with the increase in the vertical autocorrelation distance. The increase is significant for the small values

of the autocorrelation length (as compared to the embedded length of the monopile). Beyond the value of 18 m (length of the monopile), the increase in the failure probability becomes less significant. For the large values of the vertical autocorrelation length, the failure probability attains an asymptote corresponding to the case of a homogeneous soil.

## 5 Conclusions

A probabilistic analysis was performed at the Serviceability Limit State SLS for a large diameter monopile foundation in a spatially varying clay. The soil undrained cohesion was considered as a random field following a Lognormal distribution and the soil undrained Young's Modulus was assumed to be linearly related to the soil undrained cohesion. EOLE method was used for the generation of realizations of the random field.

The Global Sensitivity Analysis enhanced Surrogate (GSAS) modeling proposed by Hu & Mahadevan (2016) was extended in this work to the case of random field and used to perform the reliability analysis. The method has shown high efficiency as compared to AK-MCS since it has led to quasi similar values of the failure probability and coefficient of variation making use of a much reduced number of calls to the mechanical model.

The critical realization of the soil Young modulus exhibited some symmetry about the pivot point of the monopile. Weaker soil was observed for the depths corresponding to higher horizontal monopile displacements.

A parametric study has shown that the failure probability increases with the increase in the vertical autocorrelation distance. This increase was shown significant for a ratio of monopile embedded length to the vertical correlation length bigger than 1 ( $L/a_z > 1$ ) and tend to be negligible for the large values of the vertical autocorrelation length (as compared to the embedded length of the monopile).

## Acknowledgements

This work was carried out within the framework of the WEAMEC, West Atlantic Marine Energy Center, and with funding from the CARENE.

## References

- ABAQUS, 2016. Dassault Systèmes, Providence, RI, USA.
- API, 2000. *Recommended practice for planning, designing and constructing fixed offshore platforms—working stress design, RP2A-WSD*, 21st ed., American Petroleum Institute, Washington.
- Charlton, T.S. & Rouainia, M., 2017. A probabilistic approach to the ultimate capacity of skirted foundations in spatially variable clay. *Structural Safety*, 65, pp.126–136.
- Clausen, J., Damkilde, L. & Andersen, L., 2007. An efficient return algorithm for

- non-associated plasticity with linear yield criteria in principal stress space. *Computers and Structures*, 85, pp.1795–1807.
- DNV-OS-J101, 2014. Design of Offshore Wind Turbine Structures.
- Echard, B., Gayton, N. & Lemaire, M., 2011. AK-MCS: An active learning reliability method combining Kriging and Monte Carlo Simulation. *Struct. Saf.*, 33 (2), 145–154.
- Echard, B., Gayton, N., Lemaire, M. & Relun, N., 2013. A combined Importance Sampling and Kriging reliability method for small failure probabilities with time-demanding numerical models. *Reliab. Eng. Syst. Saf.*, 111, pp.232–240.
- Hu, Z. & Mahadevan, S., 2016. Global sensitivity analysis-enhanced surrogate (GSAS) modeling for reliability analysis. *Structural and Multidisciplinary Optimization*, pp.501–521.
- Jeong, S., Lee, J. & Lee, C.J., 2004. Slip effect at the pile-soil interface on dragload. *Comput Geotech*, 31, pp.115–126.
- Kellezi, L. & Hansen, P.B., 2003. Static and dynamic analysis of an offshore monopile windmill foundation. In *BGA International Conference on Foundations: Innovations, observations, design and practice*.
- Lacasse, S. & Nadim, F., 1996. Uncertainties in Characterising Soil Properties. In *Uncertainty in the Geologic Environment: From Theory to Practice*. Reston: ASCE, pp. 49–75.
- Lemos, L. & Vaughan, P., 2000. Clay-interface shear resistance. *Géotechnique*, 50(1), pp.55–64.
- Li, C.C. & Derkiureghian, A., 1993. Optimal discretization of random fields. *J. Eng. Mech.-ASCE*, 119 (6), pp.1136–1154.
- Li, J.H., Zhou, Y., Zhang, L.L., Tian, Y., Cassidy, M.J. & Zhang L.M., 2016. Random finite element method for spudcan foundations in spatially variable soils. *Engineering Geology*, 205, pp.146–155.
- Li, L., Li, J., Huang, J. & Gao, F., 2017. Bearing capacity of spudcan foundations in a spatially varying clayey seabed. *Ocean Engineering*, 143(July), pp.97–105.
- Lophaven, S., Nielsen, H.B. & Søndergaard, J., 2002. *DACE: A Matlab Kriging Toolbox*.
- Papazafeiropoulos, G., Muñoz-calvente, M. & Martínez-pañeda, E., 2017. Advances in Engineering Software Abaqus2Matlab : A suitable tool for finite element post-processing. *Advances in Engineering Software*, 105, pp.9–16.
- Tsubakihara, Y. & Kishida, H., 1993. Frictional behaviour between normally consolidated clay and steel by two direct shear type apparatuses. *Soils Found*, 33(2), pp.1–13.
- USACE (1990) Engineering and design: settlement analysis. Engineer manual 1110–1–1904, US Army Corps of Engineers.
- Vahdatirad, M.J., Andersen, L.V. & Ibsen, L.B., 2013. Probabilistic Three-Dimensional Model of an Offshore Monopile Foundation : Reliability Based Approach. In *Seventh International Conference on Case Histories in Geotechnical Engineering*.
- Xu, C. & Gertner, G., 2007. Extending a global sensitivity analysis technique to models with correlated parameters. *Computational Statistics & Data Analysis*, 51, pp.5579–5590.